

Constructing Acceleration Continuous Tool Paths Using Pythagorean Hodograph Curves

Zbyněk Šír¹ and Bert Jüttler

*Johannes Kepler University, Institute of Applied Geometry,
Altenberger Str. 69, 4040 Linz, Austria.*

Abstract

Any set of C^2 planar boundary data (two points with associated velocities and acceleration vectors) can be interpolated by a PH curve of degree 9. In the generic case there are four such curves [5]. In this paper we give a detailed description and a qualitative analysis of these solutions. In particular we label the four solutions and compare their fairness from the point of view of possible application. For this purpose we consider the Hermite data taken from an analytical curve and study the behavior of the solutions for decreasing step-size h . This allows us to identify explicitly the solution which – for sufficiently small step-size – matches the shape of the curve with a high precision (the approximation order is 6). Consequently we are able to develop a highly robust, fast and precise algorithm converting analytical curves or curves described in G-code into a C^2 continuous PH spline curve of degree 9.

Key words: Pythagorean Hodograph curves, CNC machining, tool path design, approximation order, Taylor expansion

1 Introduction

Traditionally, the tool paths for CNC machining are described by so-called G-code [16], which interpolates discrete tool positions along linear and circular segments. Standard real-time CNC interpolators, which evaluate the precise tool positions according to a given frequency, rely almost exclusively on the G-code. This approach is geometrically simple and the tool speed can be easily controlled along the line and circle segments.

On the other hand, this technique may also cause some complications. For example, shapes are designed in CAD systems using various free-form shapes, which must then be approximated by G code. This may lead to problems with inaccuracies and also increases the data volume. In addition, the use of circular and linear segments can ensure only the speed continuity,

¹ Corresponding author. E-mail: zbynek.sir@jku.at, tel.: +43 (0) 732-2468-9178, fax: +43 (0) 732-2468-9142, www.ag.jku.at.

Table 1

Hermite interpolation of planar data by PH curves.

data	degree	maximum number of solutions and computational effort	available results
G^1	3	2 solutions, quadratic equation (Walton and Meek [21])	One of the solutions has approximation order 4 at generic points (Walton and Meek [21]).
C^1	5	4 solutions, quadratic equations (Farouki and Neff [8])	The best solution can be identified via its rotation index (Moon et al. [18]). One of the solutions has approximation order 4 (Feichtinger [11]).
G^2	5	System of two degree 6 equations (Farouki et al. [5])	none.
$G^2[C^1]$	7	8 solutions, quartic equations (Jüttler [14])	One of the solutions has approximation order 6 at generic points [14]. Inflections reduce the approximation order.
C^2	9	4 solutions, quadratic equations (Farouki et al. [5])	The best solution can be found by “visual inspection of the curves and their control points” (Farouki et al. [5]). One of the solutions has approximation order 6 (this paper).

but the acceleration will always be discontinuous, therefore limiting the possible speed of the machinery.

Based on spline curves, various free-form curve interpolators for CNC machining have been proposed, e.g. [13,15,19,22,23]. As a major inconvenience, the arc length along these curves has to be approximated by using numerical integration.

An elegant technique for addressing this issue has been proposed by Farouki and Sakkalis, see [3] and the references cited therein. They introduced the class of *Pythagorean Hodograph* (PH) curves, which are distinguished by having a polynomial arc length function and rational offset curves. Therefore these curves provide an elegant solution of various difficult problems occurring in applications, in particular in the context of CNC machining. Various aspects of applications were studied by Farouki and several co-authors, see e.g. [6,7,10,20].

An essential step of the application of PH curves is their construction from certain input data. Due to the special algebraic properties of PH curves, all constructions – which are linear in the case of standard Bézier curves – become *nonlinear* in the PH case. In particular, the applicability of global constructions, such as global spline interpolation [4] and least-squares fitting [9], is limited, since they lead to large systems of nonlinear equations.

Local techniques seem to be more promising. Various constructions of planar PH curves matching given Hermite boundary data were developed, see table 1. For more references the

reader is referred to [3], which also includes the case of spatial curves.

This paper is devoted to the case of C^2 boundary data, which has also been addressed in [5], as a tool for design of rational CAM profiles. The authors describe the system of complex equations, which is to be solved in order to construct the PH Hermite interpolants, and show, that in general there are four such PH interpolants. After recalling some basic facts about PH curves (Section 2) and C^2 Hermite interpolation (Section 3), we discuss in Section 4 the explicit labeling of the four PH interpolants. The results are used for a qualitative analysis (Section 5). Finally, we apply the previous results and formulate algorithms for converting piecewise analytical curves and curves designed in G -code into piecewise PH curves (Section 6).

2 Preliminaries

The *hodograph* of a planar polynomial curve $\mathbf{p}(t) = [x(t), y(t)]^\top$ of degree n is the curve $\mathbf{h}(t) = [x'(t), y'(t)]^\top$ of degree $n - 1$, where $'$ denotes the first derivative. Recall that a Bézier curve is called *Pythagorean Hodograph (PH)* if the length of its tangent vector depends in a (piecewise) polynomial way on the parameter. In particular $\mathbf{p}(t) = [x(t), y(t)]^\top$ is called *planar PH curve* if there exists a polynomial $\sigma(t)$ such that

$$x'(t)^2 + y'(t)^2 = \sigma^2(t). \quad (1)$$

Solutions of eq. (1) (also called Pythagorean triplets) in unique factorization domains (which includes the ring of polynomials) were characterized by Kubota [17].

According to Farouki [2], this result can be formulated using complex numbers (see also [1] for a more general framework). Any vector $\mathbf{u} = [v, w]^\top$ is identified with the complex number $\mathbf{u} = v + iw$, and any planar polynomial curve $\mathbf{p}(t) = [x(t), y(t)]^\top$ is identified with the complex-valued function $\mathbf{p}(t) = x(t) + iy(t)$.

The PH curves are characterized as follows.

Lemma 1 *Let $\mathbf{p}(t) = x(t) + iy(t)$ be a planar polynomial curve, such that $\gcd(x'(t), y'(t))$ is a square of a polynomial¹. Then $\mathbf{p}(t)$ is PH if and only if there exists a complex polynomial $\mathbf{w}(t)$ such that the hodograph $\mathbf{h}(t) = x'(t) + iy'(t)$ satisfies $\mathbf{h}(t) = \mathbf{w}(t)^2$. The arc length function of the PH curve is a polynomial obtained by integrating $|\mathbf{w}(t)|^2$.*

Consequently, the construction of a PH curve essentially reduces to the construction of a suitable curve $\mathbf{w}(t)$. This curve will be called the *preimage*. Clearly, two complex preimages $\mathbf{w}(t)$, $\tilde{\mathbf{w}}(t)$ correspond to the same hodograph if and only if

$$\mathbf{w}(t) = \pm \tilde{\mathbf{w}}(t). \quad (2)$$

¹ This includes the generic case $\gcd(x'(t), y'(t)) = 1$.

Since two curves $\mathbf{p}(t)$, $\tilde{\mathbf{p}}(t)$ have the same hodograph if and only if they differ only by translation, a planar PH curve $\mathbf{p}(t)$ is fully determined by the preimage $\mathbf{w}(t)$ and by the location of its starting point $\mathbf{p}(0)$.

3 Construction of C^2 interpolants

We construct a planar PH curve $\mathbf{p}(t)$ which matches given C^2 Hermite boundary data. More precisely, the curve is to interpolate the end points \mathbf{P}_0 , \mathbf{P}_1 , the velocity vectors \mathbf{V}_0 , \mathbf{V}_1 and the acceleration vectors \mathbf{A}_0 , \mathbf{A}_1 at $t = 0$ and $t = 1$, respectively. We consider all this data as complex numbers.

The position of \mathbf{P}_0 can be matched by a suitable choice of the integration constant. The remaining 5 conditions (over \mathbb{C}) must be satisfied by choosing the control points of the preimage $\mathbf{w}(t)$. Consequently, the degree of $\mathbf{w}(t)$ has to be 4. This choice leads to a PH curve of degree $2 \cdot 4 + 1 = 9$.

We shall use the Bernstein-Bézier representation [12] of the hodograph $\mathbf{h}(t) = \mathbf{p}'(t)$ and the preimage $\mathbf{w}(t)$:

$$\mathbf{h}(t) = \sum_{i=0}^8 \mathbf{h}_i B_i^8(t), \quad \mathbf{w}(t) = \sum_{i=0}^4 \mathbf{w}_i B_i^4(t) \quad t \in [0, 1] \quad (3)$$

with control points $\mathbf{h}_i, \mathbf{w}_i \in \mathbb{C}$ and Bernstein polynomials $B_j^n(t) = \binom{n}{j} t^j (1-t)^{n-j}$. The interpolation conditions lead to the equations

$$\mathbf{h}_0 = \mathbf{V}_0, \quad \mathbf{h}_8 = \mathbf{V}_1, \quad 8(\mathbf{h}_1 - \mathbf{h}_0) = \mathbf{A}_0, \quad 8(\mathbf{h}_8 - \mathbf{h}_7) = \mathbf{A}_1, \quad \text{and} \quad \frac{1}{9} \sum_{i=0}^8 \mathbf{h}_i = (\mathbf{P}_1 - \mathbf{P}_0),$$

which have to be satisfied by the control points of the hodograph. After expressing them in terms of the control points of the preimage curve, one arrives at the following non-linear system of equations:

$$\mathbf{w}_0^2 = \mathbf{V}_0, \quad \mathbf{w}_4^2 = \mathbf{V}_1, \quad (4)$$

$$8\mathbf{w}_0(\mathbf{w}_1 - \mathbf{w}_0) = \mathbf{A}_0, \quad 8\mathbf{w}_4(\mathbf{w}_4 - \mathbf{w}_3) = \mathbf{A}_1, \quad \text{and} \quad (5)$$

$$\begin{aligned} & \frac{1}{9} \mathbf{w}_0^2 + \frac{1}{21} \mathbf{w}_0 \mathbf{w}_2 + \frac{1}{9} \mathbf{w}_0 \mathbf{w}_1 + \frac{1}{63} \mathbf{w}_0 \mathbf{w}_3 + \frac{1}{315} \mathbf{w}_0 \mathbf{w}_4 + \frac{2}{35} \mathbf{w}_2^2 + \frac{2}{21} \mathbf{w}_2 \mathbf{w}_1 + \frac{2}{21} \mathbf{w}_2 \mathbf{w}_3 \\ & + \frac{1}{21} \mathbf{w}_2 \mathbf{w}_4 + \frac{4}{63} \mathbf{w}_1^2 + \frac{16}{315} \mathbf{w}_1 \mathbf{w}_3 + \frac{1}{63} \mathbf{w}_1 \mathbf{w}_4 + \frac{4}{63} \mathbf{w}_3^2 + \frac{1}{9} \mathbf{w}_3 \mathbf{w}_4 + \frac{1}{9} \mathbf{w}_4^2 = (\mathbf{P}_1 - \mathbf{P}_0). \end{aligned} \quad (6)$$

Using (4) and (5), the last equation can be rewritten as

$$\begin{aligned} & (12\mathbf{w}_2 + 10\mathbf{w}_1 + 5\mathbf{w}_0 + 5\mathbf{w}_4 + 10\mathbf{w}_3)^2 = \\ & 2520(\mathbf{P}_1 - \mathbf{P}_0) - 435(\mathbf{V}_1 + \mathbf{V}_0) + \frac{45}{2}(\mathbf{A}_1 - \mathbf{A}_0) \\ & - (60\mathbf{w}_1^2 - 60\mathbf{w}_0 \mathbf{w}_3 - 60\mathbf{w}_1 \mathbf{w}_4 + 60\mathbf{w}_3^2 - 42\mathbf{w}_0 \mathbf{w}_4 - 72\mathbf{w}_1 \mathbf{w}_3). \end{aligned} \quad (7)$$

If $\mathbf{V}_0 = 0$, then $\mathbf{w}_0 = 0$ and (5) implies $\mathbf{A}_0 = 0$. Similarly, $\mathbf{V}_1 = 0$ implies $\mathbf{A}_1 = 0$. These cases, which correspond to singular points at the segment end points, will be excluded in the remainder of this paper.

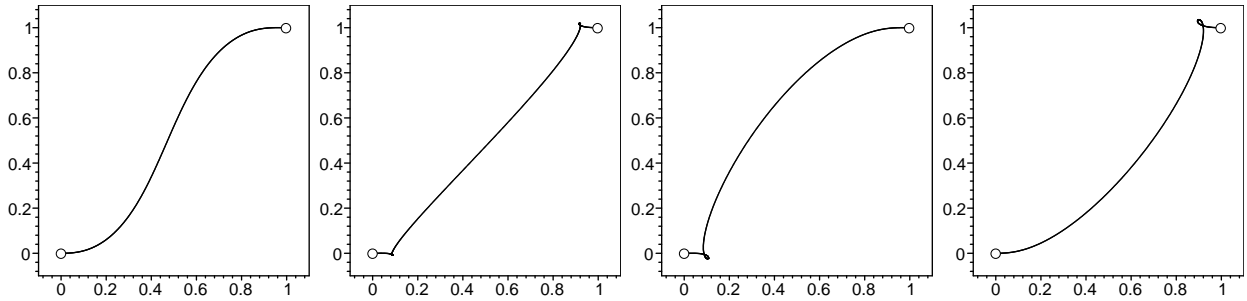


Fig. 1. Four PH interpolants of degree 9 to given C^2 Hermite data.

If both \mathbf{V}_0 and \mathbf{V}_1 are nonzero, we obtain from (4) two different solutions for \mathbf{w}_0 and two for \mathbf{w}_4 (step 1). The linear equations (5) can then be solved for \mathbf{w}_1 and \mathbf{w}_3 (step 2). Finally the quadratic equation (7) has two solutions for \mathbf{w}_2 (step 3). Therefore the system (4)-(7) has in general 8 different solutions for the preimage control points \mathbf{w}_i .

On the other hand, due to (2), always two of the computed preimages give the same PH curve. Hence, we may pick one of the two solutions for \mathbf{w}_0 and obtain 4 preimages by considering two solutions for \mathbf{w}_4 and two solutions for \mathbf{w}_2 .

Note, that for one or both choices of \mathbf{w}_4 , the right-hand side of (7) may vanish and therefore the two solutions for \mathbf{w}_2 may be identical. If this is the case, the two corresponding PH interpolants may coincide. We summarize the results in the following theorem.

Theorem 2 *The system of quadratic equations (4), (5), (7) leads to 4 planar PH curves*

$$\mathbf{p}(t) = \int \mathbf{h}(t)dt + \mathbf{P}_0 \quad (8)$$

(cf. (3)) of degree 9 interpolating the given positions $\mathbf{P}_0, \mathbf{P}_1$, the non-vanishing velocity vectors $\mathbf{V}_0, \mathbf{V}_1$ and the acceleration vectors $\mathbf{A}_0, \mathbf{A}_1$ at $t = 0$ and $t = 1$, respectively. For special configurations of the data, one or two pairs of these PH curves may coincide.

Note that the equations (4), (5), (7) characterize *all* interpolating PH curves $\mathbf{p}(t) = x(t)+iy(t)$ of degree 9 satisfying the assumption that $\gcd(x', y')$ is a square (which includes the case $\gcd(x', y') = 1$), see Lemma 1.

As an example, we consider the Hermite data

$$\mathbf{P}_0 = (0,0)^\top, \mathbf{V}_0 = (1,0)^\top, \mathbf{A}_0 = (0,1)^\top, \mathbf{P}_1 = (1,1)^\top, \mathbf{V}_1 = (1,0)^\top, \mathbf{A}_1 = (0,1)^\top, \quad (9)$$

which lead to four different PH interpolants shown on the Fig. 1. While the first solution has a reasonable shape, the other solutions are not useful, due to one or two small loops.

Remark 3 Note that additional solutions of degree 9 may exist. They can be generated by integrating a hodograph of the form

$$\mathbf{h}(t) = f(t) \mathbf{w}^2(t), \quad (10)$$

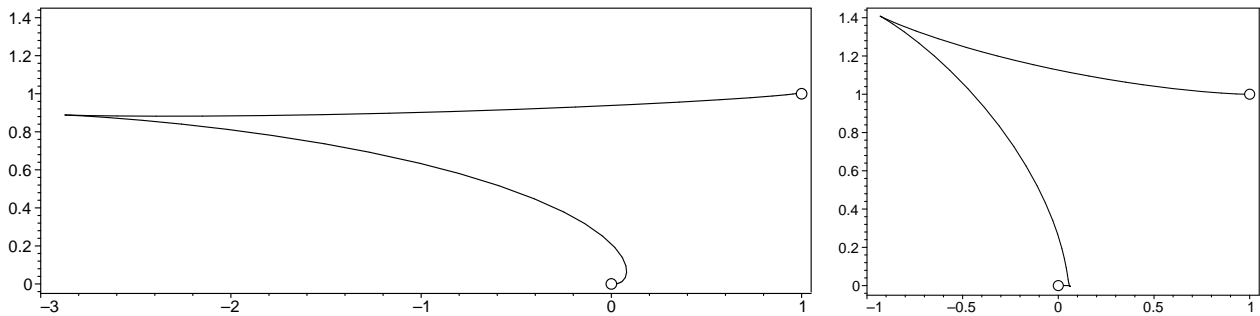


Fig. 2. Spurious interpolants for $k = 3$ (left) and $k = 2$ (right).

where $\mathbf{w}(t)$ is a complex polynomial of degree k ($k = 0, 1, 2, 3$) and $f(t)$ is a real polynomial of degree $8 - 2k$. These curves have the same number of degrees of freedom than the curves discussed in Theorem 2, which covers the case $k = 4$.

However, construction of these "spurious" interpolants is much more difficult, since the resulting non-linear systems of equations are rather complicated and do not always have real solutions. Also, according to our experiences, they have less desirable shape properties - e.g. on Fig. 2 we show two interpolants to Hermite data (9) for $k = 3$ and $k = 2$, both having cusps. Note, that for $k = 1$ the PH curve cannot describe inflected curves and for $k = 0$ it is reduced to a straight line. Therefore the spurious interpolants may not be of much use.

4 Labeling the solutions

As observed in the the example, the four PH interpolants are not of the same quality: only the first one is free of loops and has a reasonable shape. Before we proceed to the qualitative study of the four interpolants it is necessary to label them in a suitable way.

One would expect this labeling to be *invariant* with respect to Euclidean transformations and scaling of the data and to depend *smoothly* on the input data. However, it turns out that the four PH interpolants can not be labeled in an continuous way for all possible input data. In order to demonstrate this fact, consider the first interpolant of the Hermite data (9) - see first figure of Fig. 3. We change smoothly the input data by rotating the tangent vector at the point $\mathbf{P}_0 = [1, 1]^\top$ counterclockwise. At the same time we modify smoothly the PH curve such that it interpolates the changing data. After one revolution we arrive at the fourth PH interpolant of the original data (last figure of Fig. 3).

As demonstrated by this example, the labeling cannot be smooth for all input data. This is due to the fact, that the solutions differ only by choosing one of two possible complex square roots in equations (4) and (7).

In order to obtain a geometrically invariant labeling, we consider the four PH Hermite interpolants of the Hermite data in a certain canonical position. More precisely, we assume that

$$\mathbf{P}_0 = (0, 0)^\top = 0 + i0 \quad \text{and} \quad \mathbf{V}_0 = (1, 0)^\top = 1 + i0. \quad (11)$$

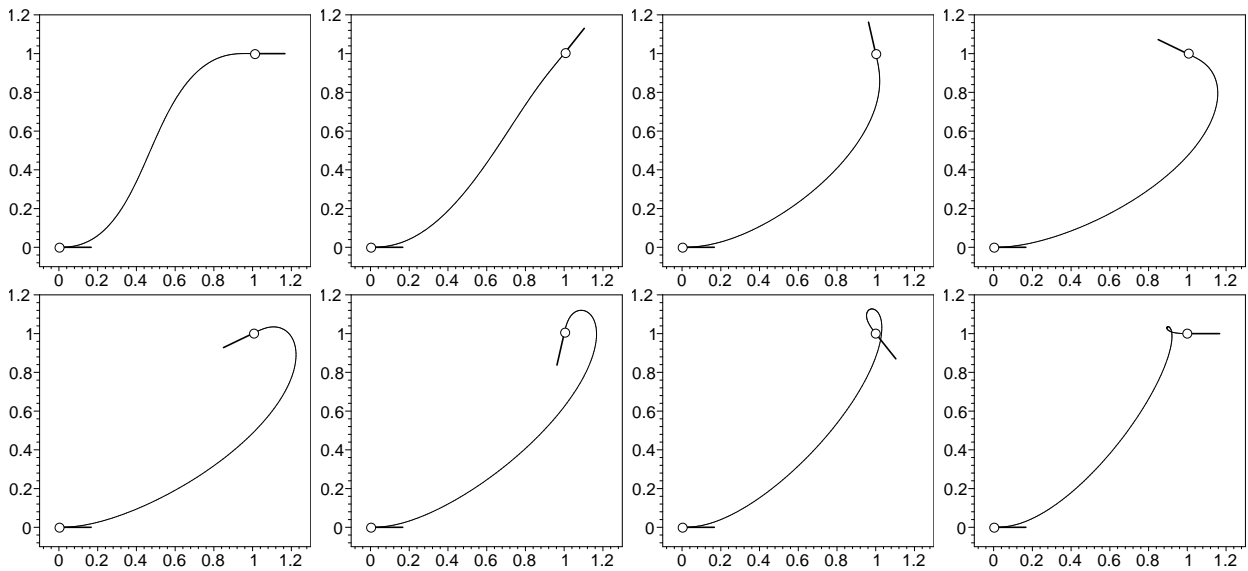


Fig. 3. A family of the PH interpolants for smoothly changing Hermite data. The end point velocity vectors have been scaled by $1/6$.

Any input data can be transformed into the canonical position by a unique similarity transformation Φ , which is composed of a translation, a rotation and a scaling. Clearly, a similarity transformation preserves the PH property, since the length of all vectors is multiplied with a constant factor. Transforming the labeled interpolants back by the inverse transformation Φ^{-1} yields an invariant labeling of the interpolants to the original data.

In the canonical position (11), the first equation (4) has two solutions $\mathbf{w}_0 = \pm 1$. Due to (2), we can pick one of the solutions, $\mathbf{w}_0 = 1$. Then the four different solutions correspond to the choice of different complex square roots while computing \mathbf{w}_4 by solving (4), and \mathbf{w}_2 by solving (7). We will label these four solutions depending on whether these square roots are chosen to have a positive or a negative real part.

For example, if $\Im(\mathbf{V}_1) \neq 0$ or $\Re(\mathbf{V}_1) > 0$, the solutions of the second equation (4) are

$$\Re(\mathbf{w}_4) = \pm \sqrt{\frac{\sqrt{\Re(\mathbf{V}_1)^2 + \Im(\mathbf{V}_1)^2} + \Re(\mathbf{V}_1)}{2}}, \quad \Im(\mathbf{w}_4) = \frac{\Im(\mathbf{V}_1)}{2\Re(\mathbf{w}_4)}, \quad (12)$$

where $\sqrt{\cdot}$ denotes the real square root (step 1). We may choose the sign of the real part(12), which corresponds to defining \mathbf{w}_4 as the complex square root of \mathbf{V}_1 with positive or negative real part.

Next, the equations (5) correspond to a systems of linear equations for the real and imaginary parts of $\mathbf{w}_1, \mathbf{w}_3$, which can be easily solved (step 2).

Finally the solutions of the equation (7) are expressed by taking square roots of its right-hand side (step 3), similarly to (12). Once again, one may choose a positive or negative sign when computing the real part. The labeling will fail if the right-hand side of (7) is a non-positive real number.

Table 2
Labeling the solutions

solutions	$\mathbf{p}_1(t)$	$\mathbf{p}_2(t)$	$\mathbf{p}_3(t)$	$\mathbf{p}_4(t)$
sign of $\Re(\mathbf{w}_4)$ (needed in step 1)	+	+	-	-
sign of $\Re(5\mathbf{w}_0 + 10\mathbf{w}_1 + 12\mathbf{w}_2 + 10\mathbf{w}_3 + 5\mathbf{w}_4)$ (needed in step 3)	+	-	+	-

The four PH curves solving the interpolation problem will be labeled as described in Table 2.

Remark 4 If \mathbf{V}_1 or the right-hand side of the equation (7) is a negative real number, than the labeling fails. In this situation, both square roots are imaginary numbers and the labeling have to become discontinuous. For this reason, we do not label the solutions in this case. If the labeling exists, then it depends smoothly on the input data.

5 Asymptotic behavior of the interpolants

In order to gain some insight into the quality of the solutions, we will now study the asymptotic behavior of the four solutions of the C^2 Hermite interpolation algorithm. More precisely, we assume that the C^2 Hermite data are taken from a small segment of an analytical curve, and we investigate the asymptotic behavior of the solutions for decreasing step-size.

We assume that the curve is given by its Taylor expansion in the canonical position (11),

$$\mathbf{C}(T) = (T + \sum_{i=2}^{\infty} \frac{x_i}{i!} T^i, \sum_{i=2}^{\infty} \frac{y_i}{i!} T^i)^\top \quad (13)$$

with arbitrary coefficients x_2, x_3, \dots and y_2, y_3, \dots

For any step-size h , we pick the segment $\mathbf{c}(t) = \mathbf{C}(ht)$, $t \in [0, 1]$. This segment has the expansion

$$\mathbf{c}(t) = (th + \sum_{i=2}^{\infty} \frac{x_i}{i!} t^i h^i, \sum_{i=2}^{\infty} \frac{y_i}{i!} t^i h^i)^\top. \quad (14)$$

Now we interpolate the C^2 Hermite boundary data at the points $\mathbf{c}(0) = \mathbf{C}(0)$ and $\mathbf{c}(1) = \mathbf{C}(h)$. Depending on the interval size h , the four different PH curves interpolating the data behave as described in the following Theorem.

Theorem 5 *The four interpolating PH curves have the Taylor expansions shown in Table 3. Among them, only the first solution \mathbf{p}_1 matches the shape of the original curve \mathbf{c} . In addition, it can be shown that*

$$\max_{t \in [0,1]} \|\mathbf{c}(t) - \mathbf{p}_1(t)\| = \mathcal{O}(h^6),$$

i.e., the approximation order of this solution is equal to six.

Proof. We derive Taylor expansions of the Hermite boundary data at $t = 0$ and $t = 1$ of the

Table 3

Taylor expansions of the four solutions

solution	leading terms of the Taylor expansion
$\mathbf{P}_1(t)$	$\begin{pmatrix} th + \mathcal{O}(h^2) \\ \frac{1}{2}t^2y_2h^2 + \mathcal{O}(h^3) \end{pmatrix}$
$\mathbf{P}_2(t)$	$\begin{pmatrix} (196t^9 - 882t^8 + 1512t^7 - 1176t^6 + 336t^5 + 42t^4 - 28t^3 + t)h + \mathcal{O}(h^2) \\ (98t^9 - 441t^8 + 756t^7 - 595t^6 + 189t^5 - 7t^3 + \frac{1}{2}t^2)y_2h^2 + \mathcal{O}(h^3) \end{pmatrix}$
$\mathbf{P}_3(t)$	$\begin{pmatrix} (36t^9 - 144t^8 + 208t^7 - 128t^6 + 36t^5 - 16t^4 + 8t^3 + t)h + \mathcal{O}(h^2) \\ (30t^9 - 123t^8 + 182t^7 - \frac{335}{3}t^6 + 23t^5 - 4t^4 + \frac{11}{3}t^3 + \frac{1}{2}t^2)y_2h^2 + \mathcal{O}(h^3) \end{pmatrix}$
$\mathbf{P}_4(t)$	$\begin{pmatrix} (36t^9 - 180t^8 + 352t^7 - 320t^6 + 108t^5 + 20t^4 - 16t^3 + t)h + \mathcal{O}(h^2) \\ (6t^9 - 33t^8 + 74t^7 - \frac{245}{3}t^6 + 41t^5 - 4t^4 - \frac{7}{3}t^3 + \frac{1}{2}t^2)y_2h^2 + \mathcal{O}(h^3) \end{pmatrix}$

curve (14):

$$\mathbf{P}_0 = \begin{pmatrix} 0 \\ 0 \end{pmatrix}, \quad \mathbf{V}_0 = \begin{pmatrix} h \\ 0 \end{pmatrix}, \quad \mathbf{A}_0 = \begin{pmatrix} x_2h^2 \\ y_2h^2 \end{pmatrix}, \quad \mathbf{P}_1 = \begin{pmatrix} h + \frac{1}{2}x_2h^2 + \frac{1}{6}x_3h^3 + \dots \\ \frac{1}{2}y_2h^2 + \frac{1}{6}y_3h^3 + \dots \end{pmatrix} \quad (15)$$

and

$$\mathbf{V}_1 = \begin{pmatrix} h + x_2h^2 + \frac{1}{2}x_3h^3 + \dots \\ y_2h^2 + \frac{1}{2}y_3h^3 + \dots \end{pmatrix}, \quad \mathbf{A}_1 = \begin{pmatrix} x_2h^2 + x_3h^3 + \dots \\ y_2h^2 + y_3h^3 + \dots \end{pmatrix}. \quad (16)$$

By comparing the coefficients in equations (4)-(7) with the help of a suitable computer algebra tool, we derive expansions of the control points \mathbf{w}_i of the four solutions. For example, in the case of the first solutions \mathbf{p}_1 we obtain:

$$\mathbf{w}_0 = \begin{pmatrix} \sqrt{h} \\ 0 \end{pmatrix}, \quad \mathbf{w}_1 = \sqrt{h} \begin{pmatrix} 1 + \frac{x_2}{8}h \\ \frac{y_2}{8}h \end{pmatrix}, \quad \mathbf{w}_2 = \sqrt{h} \begin{pmatrix} 1 + \frac{x_2}{4}h + \frac{2x_3 - x_2^2 + y_2^2}{48}h^2 + \dots \\ \frac{y_2}{4}h + \frac{y_3 - y_2x_2}{24}h^2 + \dots \end{pmatrix} \quad (17)$$

and

$$\mathbf{w}_3 = \sqrt{h} \begin{pmatrix} 1 + \frac{3x_2}{8}h + \frac{2x_3 + x_2^2 - y_2^2}{16}h^2 + \dots \\ \frac{3y_2}{8}h + \frac{y_3 - y_2x_2}{8}h^2 + \dots \end{pmatrix}, \quad \mathbf{w}_4 = \sqrt{h} \begin{pmatrix} 1 + \frac{x_2}{2}h + \frac{2x_3 - x_2^2 + y_2^2}{8}h^2 + \dots \\ \frac{y_2}{2}h + \frac{y_3 - y_2x_2}{4}h^2 + \dots \end{pmatrix} \quad (18)$$

In order to check that the labeling procedure does not fail (as described in Remark 4), it is sufficient to verify, that the real part of \mathbf{V}_1 , and of the right-hand side of (7) are positive for sufficiently small h . This is obvious for \mathbf{V}_1 from (16). The right-hand side of (7) depends of the sign choice for \mathbf{w}_4 . If "+" is chosen, then it has the Taylor expansion

$$\begin{pmatrix} 1764h + 882x_2h^2 + \frac{1008x_3 + 63y_2^2 - 63x_2^2}{4}h^3 + \mathcal{O}(h^4) \\ 882y_2h^2 + \frac{504y_3 - 63y_2x_2}{2}h^3 + \mathcal{O}(h^4) \end{pmatrix}. \quad (19)$$

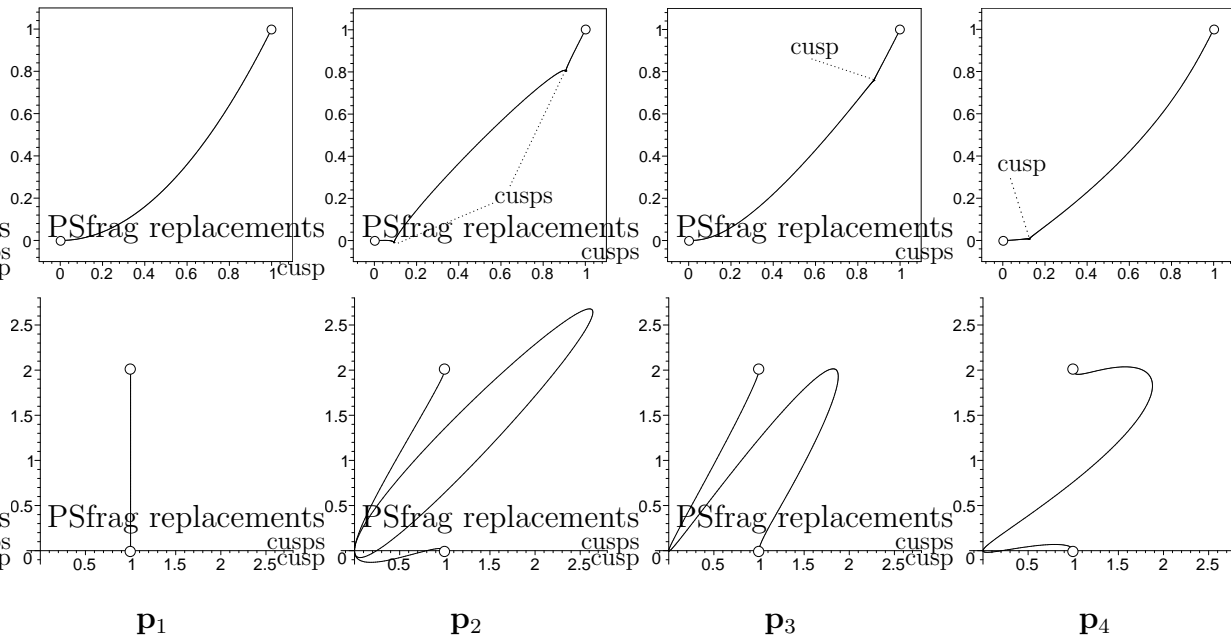


Fig. 4. Asymptotical shapes of the four solutions (top row) and of their hodographs (bottom row). The units of the coordinate axes are chosen as h (horizontal axis) and $\frac{1}{2}y_0h^2$ (vertical axis).

If “-” is chosen, then it has the Taylor expansion

$$\begin{pmatrix} 1296h + 648x_2h^2 + (168x_3 - 12y_2^2 + 12x_2^2)h^3 + O(h^4) \\ 648y_2h^2 + (168y_3 + 24y_2x_2)h^3 + O(h^4) \end{pmatrix}. \quad (20)$$

In both cases, the leading term of the real part is positive. Consequently, the labeling of the solutions is correct for sufficiently small step-size h .

Using the expansions for the control points \mathbf{w}_i , we obtain the Taylor expansions of the hodographs and of the PH interpolants, as listed in the Table 3. By considering the higher order terms, it can be shown that the first six coefficients of $\mathbf{c}(t)$ and of $\mathbf{p}_1(t)$ are identical. \square

The leading terms of the expansions shown in Table 3 define the *asymptotic shapes* of the four PH interpolants, which are shown on the Figure 4, upper row. For sufficiently small step-size h , the curves will become more and more similar to these shapes. They match very nicely the four Hermite interpolants in Figure 1. Note that the loops degenerate to cusps in the limit.

While the shape of the first solution \mathbf{p}_1 is free of singularities and reproduces the shape of the curve \mathbf{c} , the remaining three solutions have shapes involving one or two cusps, as can be clearly seen from their hodographs (second row).

This fact has an important consequence for applications: In any algorithm based on subdivision, the solution \mathbf{p}_1 must be used. Interpolation by the other solutions would not improve under subdivision. On the contrary, it would produce more and more points with very low

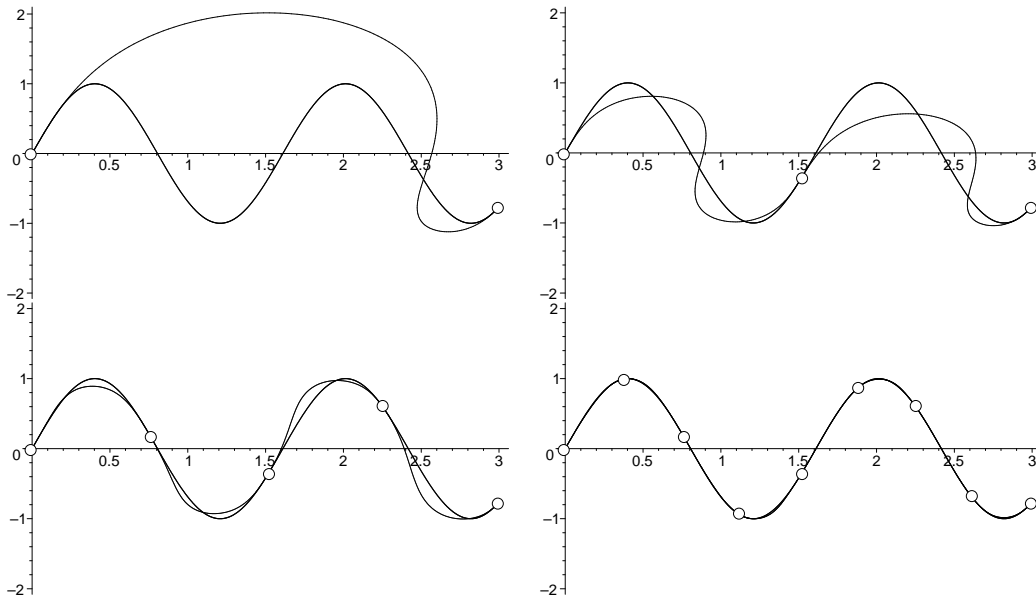


Fig. 5. Approximate conversion of an analytical curve via C^2 Hermite interpolation by PH curves, obtained after splitting the parameter domain into 1, 2, 4 and 8 segments.

parametric speed and high acceleration.

6 Conversion algorithms

As an application of the results, we discuss the conversion of arbitrary curves into PH form, and the rounding of curves described by G-code.

6.1 Analytical curves

The result described in Theorem 5 allows us to design an algorithm for the conversion of any analytical curve into a piecewise PH curve. Suppose, that the parameter domain of the analytical curve is $[0, 1]$. We split this interval into 2^n subintervals $[\frac{i}{2^n}, \frac{i+1}{2^n}]$, $i = 0..(2^n - 1)$. For each subinterval, we construct the PH Hermite interpolant \mathbf{p}_1 and obtain a C^2 continuous PH spline curve of degree 9. If the error from the original analytical curve is not sufficiently small, we continue the subdivision. Due to the Proposition 5, the error will converge to 0 as $\mathcal{O}\left(\frac{1}{64^n}\right)$ under subdivision.

The high rate of convergence is demonstrated by the following example. The figure 5 shows the segment of the analytical curve $\mathbf{c}(t) = (3t, \sin(11.7t))^\top$, $t \in [0, 1]$. We construct the PH Hermite interpolant for the whole segment and the piecewise PH interpolants obtained after splitting the parameter into 2, 4 and 8 subintervals.

This method can easily be adapted to the case of piecewise analytical curves (such as any type of NURBS curves), where the curve should first be split into its analytical segments. Also, it can be modified to use an adaptive subdivision, by splitting only those segments

where the error is still too large.

6.2 Rounding G-code curves

Many CNC controllers use G-code for the tool path description. The curves representing the tool path are composed of straight line segments and circular arcs. An important advantage of this description is the possibility to control the speed of the moving tool along the path, since the arc-length is known exactly. The main disadvantage is impossibility to obtain a motion with continuous acceleration.

In order to avoid these discontinuities we propose to smooth the G-code curve, by replacing the C^1 joints between segments by small pieces of PH curves. They are obtained by C^2 Hermite interpolation of data taken at two segments close to the joint.

Suppose that we have two neighboring segments, $\mathbf{l}(s)$ and $\mathbf{r}(s)$, both parameterized by the arc-length and having a joint at $s = s_0$. For a fixed $h > 0$ we consider the restricted segments

$$\mathbf{l}(s), \quad s \in [s_0 - h, s_0] \quad \text{and} \quad \mathbf{r}(s), \quad s \in [s_0, s_0 + h]. \quad (21)$$

We may re-parameterize the union of these two restricted segments over the interval $t \in [0, 1]$ by setting $s = 2th - h + s_0$. Finally, we construct the PH curve $\mathbf{p}_1(t)$ which interpolates the Hermite data

$$\mathbf{P}_0 = \mathbf{l}(0), \quad \mathbf{V}_0 = \mathbf{l}'(0), \quad \mathbf{A}_0 = \mathbf{l}''(0), \quad \mathbf{P}_1 = \mathbf{r}(1), \quad \mathbf{V}_1 = \mathbf{r}'(1), \quad \mathbf{A}_1 = \mathbf{r}''(1). \quad (22)$$

The error generated by this procedure is analyzed in the following proposition.

Proposition 6 *Let \mathbf{p}_1 be the first PH interpolant of the C^2 Hermite data, (22). Then*

$$\max \left\{ \max_{t \in [0, \frac{1}{2}]} \|\mathbf{l}(t) - \mathbf{p}_1(t)\|, \max_{t \in [\frac{1}{2}, 1]} \|\mathbf{r}(t) - \mathbf{p}_1(t)\| \right\} = \mathcal{O}(h^2). \quad (23)$$

Proof. The proof is again based on the Taylor expansion with respect to h . As the interpolation construction is invariant under Euclidean transformations, we may suppose that the two segments $\mathbf{l}(s)$ and $\mathbf{r}(s)$ are two circular segments with radii R_l and R_r and centers $[R_r, 0]$ and $[R_l, 0]$, having joint for $s = 0$ at $[0, 0]$,

$$\mathbf{l}(s) = \begin{pmatrix} R_l \sin\left(\frac{s}{R_l}\right) \\ R_l - R_l \cos\left(\frac{s}{R_l}\right) \end{pmatrix} \quad \text{and} \quad \mathbf{r}(s) = \begin{pmatrix} R_r \sin\left(\frac{s}{R_r}\right) \\ R_r - R_r \cos\left(\frac{s}{R_r}\right) \end{pmatrix}. \quad (24)$$

The joints linear/circular or circular/linear are included as the limit cases $R_l \rightarrow \infty$ and $R_r \rightarrow \infty$, respectively.

After the re-parameterization $s = 2th - h$, we obtain the Taylor expansions

$$\mathbf{P}_0 = \begin{pmatrix} -h + \frac{1}{6R_l^2}h^3 + \dots \\ \frac{1}{2R_l}h^2 + \dots \end{pmatrix}, \mathbf{V}_0 = \begin{pmatrix} 2h - \frac{1}{R_l^2}h^3 + \dots \\ -\frac{2}{R_l}h^2 + \dots \end{pmatrix}, \mathbf{A}_0 = \begin{pmatrix} \frac{4}{R_l^2}h^3 + \dots \\ \frac{4}{R_l}h^2 + \dots \end{pmatrix} \quad (25)$$

and

$$\mathbf{P}_1 = \begin{pmatrix} h - \frac{1}{6R_r^2}h^3 + \dots \\ \frac{1}{2R_r}h^2 + \dots \end{pmatrix}, \mathbf{V}_1 = \begin{pmatrix} 2h - \frac{1}{R_r^2}h^3 + \dots \\ \frac{2}{R_r}h^2 + \dots \end{pmatrix}, \mathbf{A}_1 = \begin{pmatrix} -\frac{4}{R_r^2}h^3 + \dots \\ \frac{4}{R_r}h^2 + \dots \end{pmatrix}. \quad (26)$$

of the Hermite data (22). Similarly the proof of the Theorem 5, we generate Taylor expansions of the preimage, of the hodograph and of the PH interpolant \mathbf{p}_1 . Finally we obtain the expansions of the errors

$$\begin{aligned} \|\mathbf{l}(t) - \mathbf{p}_1(t)\| &= \frac{1}{2} \left| \frac{1}{R_l} - \frac{1}{R_r} \right| (1-2t)(2-t)t^3h^2 + \dots \quad \text{and} \\ \|\mathbf{r}(t) - \mathbf{p}_1(t)\| &= \frac{1}{2} \left| \frac{1}{R_l} - \frac{1}{R_r} \right| (2t-1)(1+t)(1-t)^3h^2 + \dots, \end{aligned} \quad (27)$$

which conclude the proof. Note that if $R_l = R_r$ holds, then the joint becomes analytic and the approximation order of the error will be 6. \square

By analyzing the leading terms of (27), one gets

$$\max_{t \in [0, \frac{1}{2}]} \frac{(1-2t)(2-t)t^3}{2} = \max_{t \in [\frac{1}{2}, 1]} \frac{(2t-1)(1+t)(1-t)^3}{2} = \frac{36}{125} \sqrt{10} - \frac{9}{10} \approx 0.0107 \quad (28)$$

While it is rather difficult to obtain an explicit bound for the interpolation error due to the influence of the higher order terms of the Taylor expansions (27), it would be highly useful to have an a priori error bound. We propose the following bound obtained by majoring certain coefficients in the Taylor expansion (27).

Conjecture 7 *If $h < \frac{1}{2}\pi \min(|R_l|, |R_r|)$, then the error of replacing the segment joint by the first PH interpolant to the points at arc-length distance h from the joint is bounded by*

$$0.016 \left| \frac{1}{R_l} - \frac{1}{R_r} \right| h^2 + \frac{0.004 h^6}{(|R_l| + |R_r|)^5}. \quad (29)$$

Experiments with about 30,000 various input data R_l , R_r and h confirmed correctness of this bound and showed it to be very conservative (the real error was always in between this bound and its half). The h^6 term is necessary only for the cases when $R_l \approx R_r$ and can be omitted otherwise.

This formula allows to smooth a G-code curve with a prescribed precision in a very efficient way. We demonstrate this by an example.

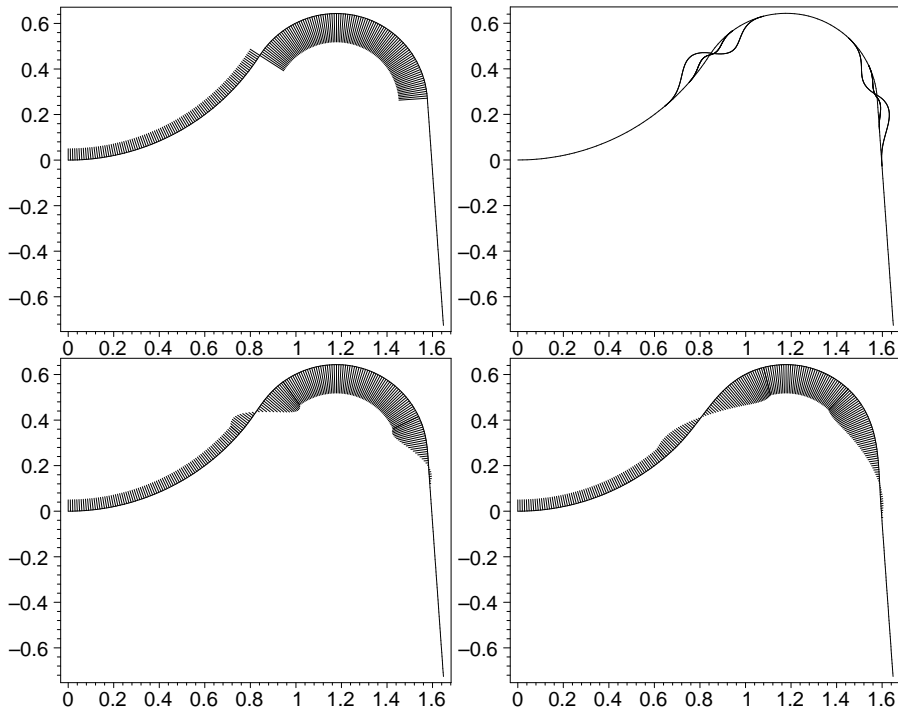


Fig. 6. A G-code curve and its acceleration vectors scaled by $1/20$ (upper left figure), and two smoothing PH curves together along with the acceleration vectors (lower figures). The three curves are also shown in the upper right figure, where the error between the original curve and their approximations has been amplified by a factor 20, in order to make it visible.

Consider the curve shown in the first figure Fig. 6, which represents a curve composed of two circular segments (with radii 1 and 0.4) and one linear segment. The vectors of instantaneous acceleration corresponding to a constant speed motion are shown (scaled by $1/20$). Note the discontinuous acceleration at the joints.

The plots in the second row show the two smoothed curves, along with the acceleration distribution. They were obtained by interpolating the circular/linear segments respectively at distance $h = 0.15$ and 0.3 from the joints. Note the high precision of the interpolation. Using (29), the maximal error is bounded by 0.0022 for $h = 0.3$ and by 0.00054 for $h = 0.15$. The shape of the interpolants can be seen in the upper right figure, where the distance of the PH curve from G-code curve is amplified by a factor 20.

As demonstrated by this example, there is a tradeoff between the error of the modified tool path (i.e., the deviation from the original G-code curve, which increases with h) and the smoothness of the acceleration (which also increases with h). In addition, one may observe a Gibbs-type phenomenon in the distribution of the acceleration (similar to the Fourier series of a discontinuous function).

7 Conclusion

We have discussed the problem of C^2 Hermite interpolation with Pythagorean hodograph curves. It has been shown, that this problem can be efficiently² be solved using curves of degree 9, and that the best solution has approximation order 6. Based on these results, we formulated algorithms for converting arbitrary curves into PH spline form, and for rounding G-code curves.

By comparing the techniques which are available for the different cases of boundary data (see Table 1), one may conclude that the use of geometric data (tangent directions and curvatures) instead of analytic ones (velocities and accelerations) does not produce any real advantage. Clearly, the degree of the resulting curves is much lower: It is 5 for G^2 data, and 7 for mixed $G^2[C^1]$ data, instead of 9 for C^2 data. However, the computation of the solution becomes more complicated, and solutions do not always exist. Moreover, the approximation order of the ‘best’ solution depends on the shape of the given curve (cf. [14], where a reduction of the approximation order has been observed at inflections), while it remains the same for all points in the case of analytic data.

In general, it can be shown, that the C^k Hermite interpolation always leads to three quadratic equations over \mathbb{C} and can be solved by PH curves of degree $4k + 1$.

Acknowledgment

The first author was supported through grant P17387-N12 of the Austrian Science Fund (FWF). The authors are indebted to the head of the CNC department at ProCom GmbH (Aachen, Germany), Dr. Elmar Wings, for the fruitful discussion concerning CNC machining, which resulted in the development of the method for rounding G-code (Section 6.2).

References

- [1] H.I. Choi, D.S. Lee and H.P. Moon (2002), Clifford algebra, spin representation, and rational parameterization of curves and surfaces. *Adv. Comput. Math.* 17, 5-48.
- [2] R.T. Farouki (1994), The conformal map $z \rightarrow z^2$ of the hodograph plane. *Comp. Aided Geom. Design* 11, 363-390.
- [3] R.T. Farouki (2002), Pythagorean hodograph curves, in G. Farin, J. Hoschek and M.-S. Kim (eds.), *Handbook of Computer Aided Geometric Design*, North-Holland, Amsterdam, 405–427.
- [4] R.T. Farouki, B.K. Kuspa, C. Manni and A. Sestini (2001), Efficient solution of the complex quadratic tridiagonal system for C^2 PH quintic splines, *Numer. Alg.* 27, 35-60.
- [5] R.T. Farouki, J. Manjunathaiah and S. Jee (1998), Design of rational cam profiles with Pythagorean-hodograph curves. *Mech. Mach. Theory* 33, 669-682.

² by evaluating six real square roots

- [6] R.T. Farouki, J. Manjunathaiah, D. Nichlas, G.F. Yuan and S. Jee (1998), Variable-feedrate CNC interpolators for constant material removal rates along Pythagorean-hodograph curves. *Comp.-Aided Design* 30 (8), 631-640.
- [7] R.T. Farouki, J. Manjunathaiah and G.-F. Yuan, G codes for the specification of Pythagorean-hodograph tool paths and associated feedrate functions on open-architecture CNC machines, *International Journal of Machine Tools and Manufacture* 39, (1999), 123-142.
- [8] R.T. Farouki and C.A. Neff (1995), Hermite interpolation by Pythagorean-hodograph quintics. *Math. Comput.* 64, 1589-1609.
- [9] R.T. Farouki and K. Saitou and Y.-F. Tsai (1998), Least-squares tool path approximation with Pythagorean-hodograph curves for high-speed CNC machining. *The Mathematics of Surfaces VIII, Information Geometers*, Winchester, 245-264.
- [10] R.T. Farouki and S. Shah (1996), Real-time CNC interpolators for Pythagorean-hodograph curves, *Computer Aided Geometric Design* 13, 583-600.
- [11] R. Feichtinger (2005), Hermite-Interpolation mit PH-Quintiken, Diplomarbeit (MSc. thesis), Johannes Kepler University, Linz, Austria, in progress.
- [12] J. Hoschek and D. Lasser (1996), *Fundamentals of Computer Aided Geometric Design*, AK Peters, Wellesley MA.
- [13] J.-T. Huang and D.C.H. Yang (1992), A generalized interpolator for command generation of parametric curves in computer controlled machines, *Proceedings of the Japan/USA Symposium on Flexible Automation*, vol. 1. ASME, 393-399.
- [14] B. Jüttler (2001), Hermite interpolation by Pythagorean hodograph curves of degree seven. *Math. Comp.* 70, 1089-1111.
- [15] Y. Koren (1976), Interpolator for a computer numerical control systems, *IEEE Transactions on Computers* C-25, 32-37.
- [16] Y. Koren (1983), *Computer Control Manufacturing Systems*, McGraw-Hill, New York.
- [17] K.K. Kubota (1973), Pythagorean Triplets in Unique Factorization Domains, *Amer. Math. Monthly* 79, 503-505 (1972).
- [18] H.P. Moon, R.T. Farouki and H.I. Choi (2001), Construction and shape analysis of PH quintic Hermite interpolants, *Comp. Aided Geom. Design* 18, 93-115.
- [19] M. Shpitalni, Y. Koren and C.C. Lo (1994), Realtime curve interpolators, *Computer Aided Design* 26, 832-838.
- [20] Y.-F. Tsai, R.T. Farouki and B. Feldman (2001), Performance analysis of CNC interpolators for time-dependent feedrates along PH curves, *Comput. Aided Geom. Design* 18, no. 3, 245-265.
- [21] D.S. Meek and D.J. Walton (1997), Geometric Hermite interpolation with Tschirnhausen cubics, *Journal of Computational and Applied Mathematics* 81, 299-309.
- [22] E. Wings and B. Jüttler (2004), Generating Tool Paths on Surfaces for a Numerically Controlled Calotte Cutting System, *Computer-Aided Design* 36, 325-331.
- [23] D.C.H. Yang and T. Kong (1994), Parametric interpolator versus linear interpolator for precision CNC machining, *Computer Aided Design* 26, 225-234.